Physical Science International Journal
7(1): 20-27, 2015, Article no.PSIJ.2015.054
ISSN: 2348-0130

SCIENCEDOMAIN *international*
www.sciencedomain.org

Effect of Gamma Radiation in Undoped SnO_2 Thin Films

A. F. Maged[1*], L. A. Nada[1] and M. Amin[2]

[1]Department of Solid State and Electron Accelerator, National Center for Radiation Research and Technology, (NCRRT), Atomic Energy Authority, P.O.Box 8029, Nasr City, Cairo, Egypt.
[2]Department of Physics, Faculty of Science, Cairo University, Giza, Egypt.

Authors' contributions

This work was carried out in collaboration between all authors. Author AFM designed the study, wrote the protocol, wrote the first draft of the manuscript and managed the literature searches, analyses of the study performed the spectroscopy analysis. Author LAN managed the experimental process and author MA identified the species of plant. All authors read and approved the final manuscript.

Article Information

DOI: 10.9734/PSIJ/2015/17250
Editor(s):
(1) Yalin Lu, Department of Physics, US Air Force Academy, USA.
(2) Preeti Singh, Department of Physics, DIT, Greater Noida (U.P.), India.
(3) Abbas Mohammed, Blekinge Institute of Technology, Sweden.
Reviewers:
(1) Mohsen Ahmadipour, School of Materials and Mineral Resources Engineering, University of Sains Malaysia, Malaysia.
(2) Anonymous, Turkey.
(3) Anonymous, Taiwan.
(4) Anonymous, Malaysia.
Complete Peer review History: http://www.sciencedomain.org/review-history.php?iid=1053&id=33&aid=9134

Original Research Article

Received 6th March 2015
Accepted 17th April 2015
Published 7th May 2015

ABSTRACT

This paper was reported on study the effect of gamma radiation on nanoporous SnO_2 electrodes for dye-sensitized solar cells. Structural, optical and electrical properties were studied. The refractive index was decreased with the increase in gamma radiation. The resistivity of thin films was decreased about 40% with the increase of gamma radiation at 659 nm film thicknesses. The mobility and carrier concentration were increased with the increase of gamma dose at 659 nm film thickness.

Keywords: SnO_2; semiconductors; thin film; radiation.

**Corresponding author: Email: magedali@hotmail.com;*

1. INTRODUCTION

Tin oxide has attracted great attention and many uses in recent decades because of its high transparency and conductivity combined with superior stability. The major applications of transparent conducting oxides include thin-film photovoltaic [1], gas sensors [2-5], optoelectronics [6], heat reflectors in solar cells windows [7]. The above-mentioned properties make them very useful in many fields of applications: Transparent electrodes for silicon and SeTe and GeSeTe alloys [8]. The ionizing radiation is available especially as gamma and determination of its effect is important for the efficient usage of devices on the satellites, space shuttles and industrial Cobalt units [9]. Glass materials are broadly used in the application areas of low-orbit satellites and spacecrafts [10]. Therefore, examination of radiation effects on the glass materials is imperative as well. These effects are associated with the energy of radiation, as well as the total dose [11].

2. EXPERIMENTAL PROCEDURE

Spray pyrolysis was a physical deposition technique where the endothermic thermal decomposition was taken place at the hot surface of the substrate to give the final product. The nano-structured films were prepared from crystalline hydrate of tin tetrachloride ($SnCl_4.5H_2O$) which had weight of 5 gm by dissolution in 5 mL pure methanol. The substrate temperature was in the range of 400–500ºC. After the deposition, the films were dried for 1 hour at room temperature. The film thickness was estimated from UV-Vis spectrophotometer, and found 191, 232, 478 and 659 nm, respectively. The deposited thin films were confirmed by X-ray diffraction examination using an X-ray diffractometer Shimadzu machine model (XD-DI series) with Cu-Kα radiation as a target, λ=1.548 Å, operated at 400 kV and 30 mA using Bragg–Brentano method. The average crystallite size was estimated from the width of x-ray lines by Scherrer's method. The optical transmittance spectra of SnO_2 films were measured in the wavelength range from 190 to 1100 nm by means of the Specord 210 plus UV-Vis spectrophotometer. The electrical properties were studied by sheet resistance method by using RCL meter at room temperature (The Philips/Fluke PM6303A RCL Meter). All measurements were made using a 4-wire technique, which ensures high-accuracy measurements, even for low-impedance components. SnO_2 films were exposed to a Co-60 gamma-radiation source with a dose rate 2.32 kGy. hr^{-1} at room temperature in National Center for Radiation Research and Technology, Egyptian Atomic Energy Authority. The selection of exposure dose was in the range 0.5-22 kGy which is based on industrial applications.

3. RESULTS AND DISCUSSION

3.1 X-Ray Analysis

It was seen that the pattern of the SnO_2 film with diffraction peaks at about positions 26.8, 35.3, 37.4 and 52.4 degree, correspond to diffraction signals produced by the (110), (101), (200) and (211) crystalline planes of the tetragonal structure of Tin element from the Joint Committee Powder Diffraction Standard (JCPDS) No. 41-1445. These peaks were increased with the increase of thickness at same positions as shown in Fig. (1). It may be due to the intensity of the diffraction peaks were determined by the arrangement of atoms in the entire crystal.

It was observed that no change in the peak intensity and position after exposing to gamma radiation up to 22 kGy as shown in Fig. (2).

Assuming a homogeneous strain across crystallites, the crystallite size of nano-crystallite was calculated from the full width half maximum (FWHM) values by using the Scherrer formula for crystallite size broadening of diffraction peaks,

$$D = \frac{0.9\,\lambda}{B\cos\theta} \quad (1)$$

Where D is crystallite size, λ is the wavelength of x-ray, B is FWHM of diffraction peak and θ is the diffraction angle. The crystallite size of tin oxide thin films was in the range of 8 and 16 nm.

3.2 Optical Band Gap

Basically, there are two types of optical transition that can occur at the fundamental edge of crystalline semiconductors: Direct and indirect transitions. For simple parabolic bands ($N(E)\ \alpha\ E^{1/2}$) and for direct transitions,

$$\alpha(\nu)n_o h\nu \approx (h\nu - E_g)^n \quad (2)$$

Where, α is the absorption coefficient n is a constant of ½ for allowed transitions and of 3/2

for forbidden transitions in the quantum-mechanical sense, n_o is the refractive index which is assumed to be a constant over energy variation, $h\nu$ is photon energy and E_g is the band gap energy of the material under investigation. This type of absorption is independent of temperature apart from any variation in E_g

There is α shift in the band gap towards higher energy for the thin film having higher carrier density. This shift was due to the filling of the states near the bottom of the conduction band [12-13]. The shift was given by the relation,

$$E_g = E_{go} + \Delta E_g^{BM} \quad (3)$$

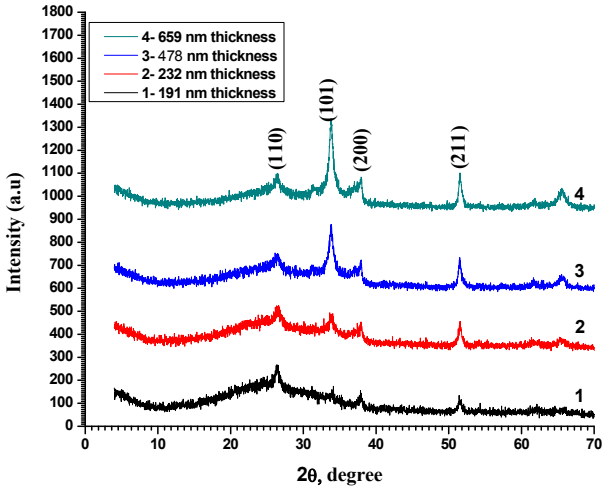

Fig. 1. Plot of x-ray diffraction spectrum at all thicknesses before gamma radiation

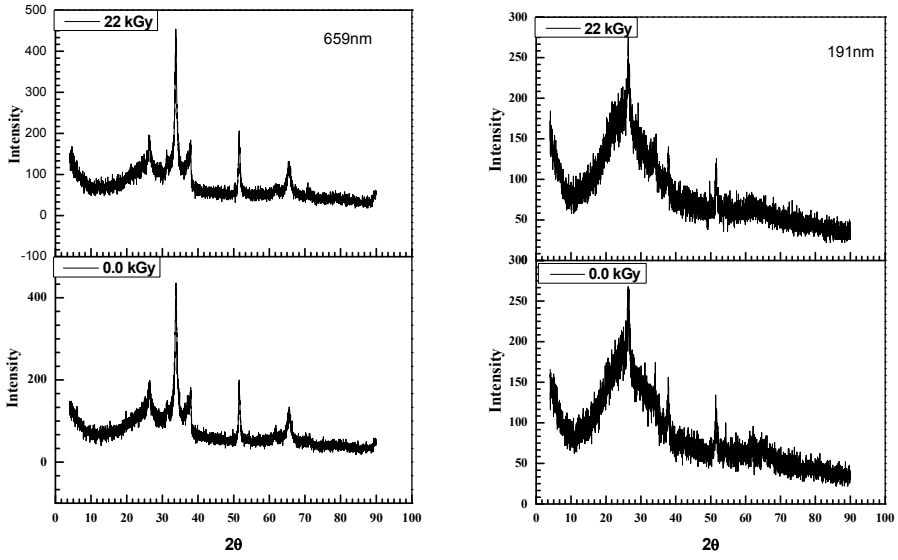

Fig. 2. Plot of x-ray diffraction spectrum at 659 and 191 nm film thicknesses before and after gamma radiation

Where E_{go} is the intrinsic band gap and ΔE_g^{BM} is the BM shift (Burstein- Moss shift). The shift is related to the carrier density as,

$$\Delta E_g^{BM} = \frac{\pi^2 h^2}{2m^*} \left(\frac{3N}{\pi}\right)^{2/3} \quad (4)$$

Where m* is the reduced effective mass and N is carrier density.

The direct transition property of SnO_2 films, Eq.2 was applied with n = 1/2 in the case of the crystalline film and with n = 2 which could be applied to amorphous film [8]. The optical properties mainly depend on the refractive index of the material and thickness of the film. The absorption and dispersion of a plane electromagnetic wave was described by the complex refractive index Ǹ = n + ik, where n is the real refractive index and k is the extinction coefficient. The physical significance of k is that on traversing a distance in the medium equal to one vacuum wavelength, the amplitude of the wave decreases by the factor $\exp(-2\pi ik)$. It was observed that the decrease in the transmission with the increase in thin film thicknesses. It may be due to the increase of opacity as shown in Fig. (3).

The transmission spectra of glass substrate (corning glass) and as deposited before and after gamma radiation exposure were shown in Fig. 4.

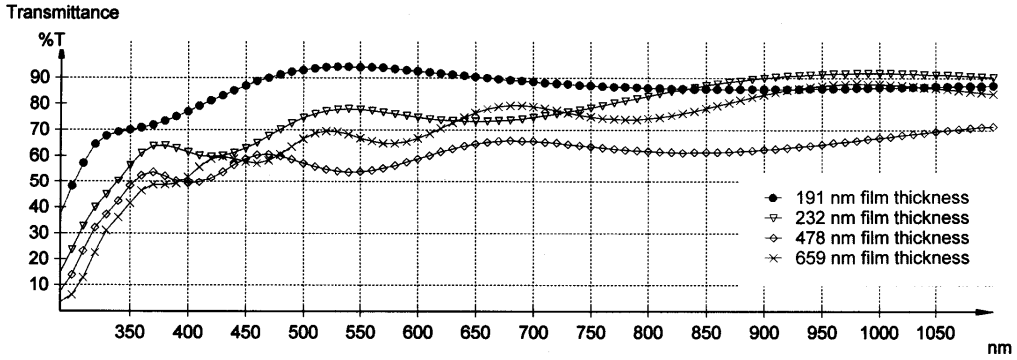

Fig. 3. Plot of transmission % as a function of wavelength for SnO_2 film of different thicknesses

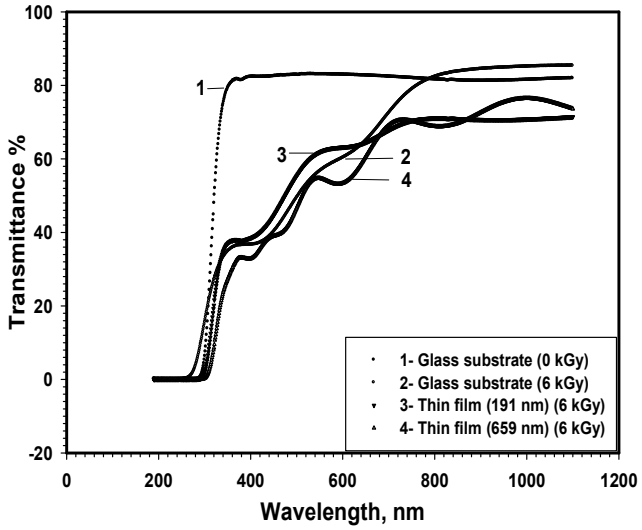

Fig. 4. Transmission spectra of glass substrate and as deposited films before and after gamma radiation

It was noticed that a decrease 63% in transmission for the glass substrate after gamma radiation exposure in visible range. This decrease might be due to that the transparent glass was converted into brown color after exposing to 6 kGy gamma dose. There was absorption coefficient, α shift at absorption edge towards higher energy with the increase of film thicknesses as shown in Fig. 5.

The absorption coefficient difference (δ) as a function of gamma dose for SnO_2 at 191 nm film thickness was shown in Fig. 6. There was an exponentially increase up to gamma dose 6 kGy then it was saturated. It could be possible to use as gamma dosimeter up to 6 kGy which is used in the industrial applications.

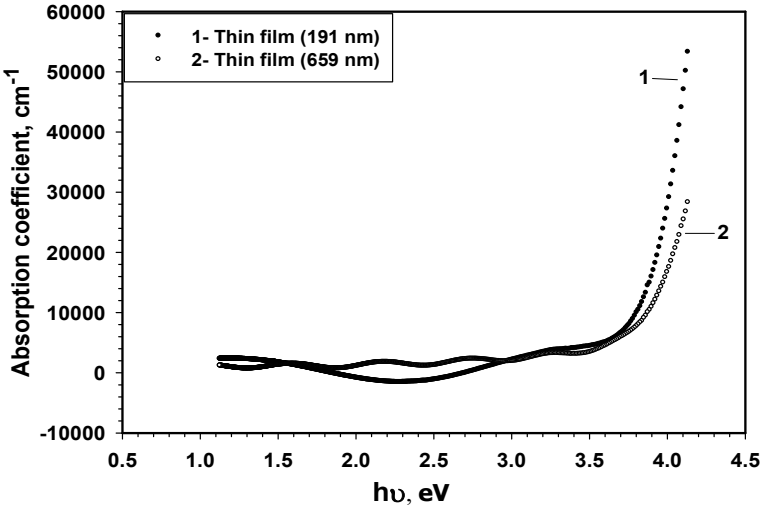

Fig. 5. Plot of absorption coefficient α vs. energy for SnO_2 at 191 and 659 nm films thickness, respectively

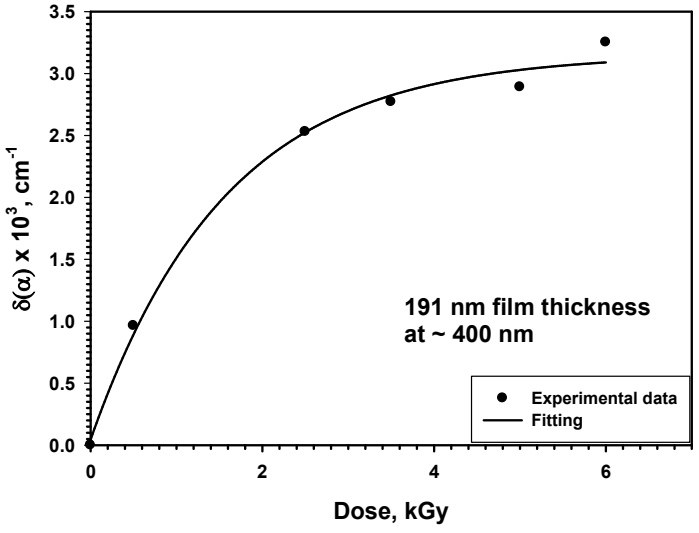

Fig. 6. Absorption coefficient difference (δ) as a function of gamma dose of selected film

The absorption coefficient, α as a function of wavelength for SnO_2 at 659 nm film thickness in the interference area was shown in Fig. 7. There was an increase in the absorption coefficient with the increase in wavelength and more increase after gamma radiation. The absorbance as a function of wavelength in the interference area before radiation (Fig. 7-1) has different orientation behavior from the radiated sample (Fig. 7-2). It might be due to the color change of glass substrate after exposing to gamma radiation. The same behavior of (α) was observed to the extinction coefficient (k).

The refractive index was decreased with the increase of wavelength before and after radiation exposure as shown in Fig. 8-A. The refractive index and extinction coefficient for the thin film at thickness range 191-659 nm were calculated in the interference area. The refractive index in this study was coincidence with atomic layer deposition method of tin oxide films [14]. The absorbance as a function of wavelength before and after radiation exposure was shown in (Fig. 8-B).

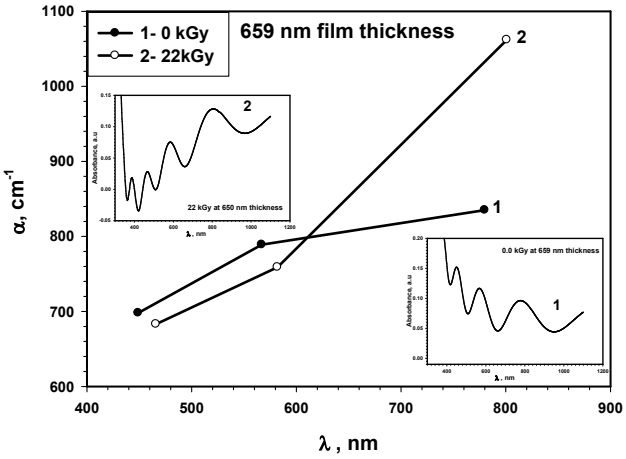

Fig. 7. The absorption coefficient, (α) vs. wavelength in the interference area of film before and after radiation

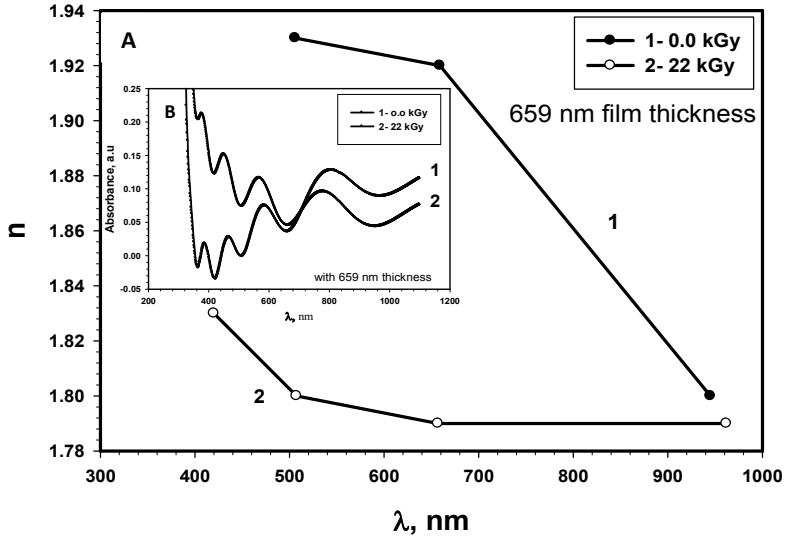

Fig. 8. The refractive index vs. wavelength in the interference area of thickness 659 nm

Our results were relatively matching the changes in the refractive index correspond to the fact that the refractive indices of SnO_2 were 1.96 and 1.79 before and after gamma radiation exposure, respectively [14-15]. The values of *k* were in the range of $1.6x10^{-2}$-$1.8x10^{-2}$ before radiation and it was found in the range $0.3x10^{-2}$–$3.2x10^{-2}$ after radiation exposure. As reported in [16] the refractive index of SnO_2 at 550 nm is 2.0 and the extinction coefficient was 0.03 and these results were relatively consistent to this work. The high absorption coefficient was observed for the SnO_2 films due to the polycrystalline of the sample, which was evident from the x-ray studies.

The direct band gap of tin oxide were reported 4.3 eV [17], 3.1 eV [18] and 3.95 eV [19]. In the present report, the direct band gap obtained was 3.88 eV at an atmospheric pressure of $1.01x10^{-5}$ Pa and room temperature before radiation and 3.96 after radiation exposure. The variation of the direct band gap with radiation for 191 and 659 nm film thicknesses were may be due to the Burstein-Moss shift.

3.3 Electrical Properties

It was found that the sheet resistance decreased from 16 kΩ/ϒ to 3 kΩ/ϒ with the increase of film thickness. The resistivity was decreased from 32×10^{-2} Ω/-cm, to 12×10^{-2} Ω-cm after radiation for 191 nm film thickness. It was found that the resistivity decreased exponentially with the increase gamma dose and it might be used as gamma dosimeter. The mobility and carrier concentration were found 1.1 cm^3/V-s and $1.9\times10^{19}/cm^3$, respectively before radiation at 191 nm film thickness. These values were found relatively consistent with the values was reported [14-15]. The mobility and carrier concentration were increased with the increase of radiation at 659 nm film thickness and it is believed that damage caused to the contact regions is responsible for this shift. Ionization is the process of removing or adding an electron to a neutral atom, thereby creating anion.

4. CONCLUSION

The structural, optical and electrical properties of SnO_2 thin films on glass substrates were evaluated before and after gamma radiation exposure. X-ray diffraction was revealed that the SnO_2 films were crystalline. A red shift in the absorption edge was observed with the increase of thickness. The thin film deposited on glass was yielded optical transmission of 94% at 191 nm film thickness. The optical energy gap was increased to 3.95 eV at gamma dose 6 kGy. There was absorption coefficient, α shift in the band gap towards higher energy for the thin film which having higher carrier density. At wavelength range $400–950$ nm, the values of extinction coefficient were in the range of 1.6 $x10^{-2}$–$1.8x10^{-2}$ before radiation and it was found in the range $0.3x10^{-2}$–$3.1x10^{-2}$ after radiation exposure. Radiation was induced changes in the optical and electrical properties of SnO_2 films resulted in the degradation of their performance.

ACKNOWLEDGEMENTS

Special thanks to Solid State and Electron Accelerator Department Staff members, EAEA, for their help of this work.

COMPETING INTERESTS

Authors have declared that no competing interests exist.

REFERENCES

1. Stefik M, Heiligtag FJ, Niederberger M, Grätzel M. Improved nonaqueous synthesis of TiO_2 for dye-sensitized solar cells. American Chemical Society, Nano. 2013;7(10):8981–8989.
2. Huang XJ, Choi YK, Yun KS, Yoon E. Oscillating behaviour of hazardous gas on tin oxide gas sensor: Fourier and wavelet transform analysis. Sensors and Actuators B Chem. 2006;115:357-364.
3. Yang H, Zhang X, Tang A. Mechanosynthesis and gas-sensing properties of n_2O_3/SnO_2nanocomposites. Nanotechnology. 2006;17:2860.
4. Simakov V, Yakusheva O, Grebennikov A, Kisin V. I–V characteristics of gas-sensitive structures based on tin oxide thin films. Sensors and Actuators B. 2006;116(1-2):221-225.
5. Jin C, Yamazaki T, Ito K, Kikuta T, Nakatani N. H_2S sensing properties of porous SnO_2 sputerred films coated with various doping films. Vacuum. 2006; 80:723-725.
6. Wang GF, Tao XM, Huang HM. Light-emitting devices for wearable flexible displays. Coloration Technology. 2005; 121:132-138.
7. Nabin Sarmah, Bryce S. Richards, Tapas K. Mallick. Evaluation and optimisation of

the optical performance of low-concentrating dielectric compound parabolic concentrator using ray-tracing Methods. Applied Optics. 2011;50(19): 3303-10.
8. Maged AF, Amin GAM, Semary M, Borham E. Metal induced effects on some physical properties of Se0.8Te0.2 amorphous system. Thin Solid Films. 2010;518:2628–2631.
9. Bhata JS, Maddani KI, Karguppikar AM, Ganesh S. Electron beam radiation effects on electrical and optical properties of pure and aluminum doped tin oxide films. Nuclear Instruments and Methods in Physics Research B. 2007;258(2):369–374.
10. Maged AF, Montasser KI, Amer HH. J. Optical absorption of amorphous semiconductors $Ge_{20}As_{30}Se_{5O-x}Te_x$ and the effect of γ-irradiation. Materials Chemistry and Physics. 1998;56/2:184-188.
11. Goswami A. Thin Film Fundamentals, New Age International (P) Limited, Publishers, New Delhi; 2003.
12. Burstein E. Anomalous Optical Absorption Limit in InSb. Physical Review. 1954; 93:632–633.
13. Moss TS. The interpretation of the properties of indium antimonide. Proceedings of the Physical Society, London, B. 1954;67:775–782.
14. Elam WJ, Baker AD, Hryn JA, Martinson BFA, Pellin JM, Hupp TJ. Atomic layer deposition of tin oxide films using tetrakis (dimethylamino) tin. Journal of Vacuum Science & Technology A. 2008;26(2):244–252.
15. Heo J, Hock AS, Gordon RG. Low temperature atomic layer deposition of tin oxide. Chemistry of Materials. 2010; 22:4964–4973.
16. Habibi MH, Talebian N. The effect of annealing on structural, optical and electrical properties of nanostructured tin doped indium oxide thin films. Acta Chimica Slovenica. 2005;52:53-59.
17. Spence W. The UV absorption edge of tin oxide films. Journal of Applied Physics. 1967;38:3767.
18. Reddy MHM, Chandorkar ANE. Beam deposited SnO, Pt-SnO and Pd-SnO, thin films for LPG detection. Thin Solid Films. 1999;349:260-265.
19. Sundaram KB, Bhagavat GK. Optical absorption studies on tin oxide films. Journal of Physics D: Applied Physics. 1981;14:921.

Peer-review history:
The peer review history for this paper can be accessed here:
http://www.sciencedomain.org/review-history.php?iid=1053&id=33&aid=9134